Electronic supplementary information

ROS and shear stress dual-sensitive bionic system with cross-linked dendrimers for atherosclerosis therapy

Meili Shen, Shunyu Yao, Shaojing Li, Xiaodong Wu, Shun Liu, Qingbiao Yang, Jianshi Du, Jingyuan Wang, Xiangyu Zheng and Yapeng Li*

Materials and method

Materials

All reactions with air and/or water-sensitive compounds were carried out under a dry nitrogen atmosphere. Methyl acrylate (GC, > 99.0%, containing ≤100 ppm MEHQ stabilizer), 2-iminothiolane hydrochloride (98%), bovine albumin (BSA), Fluorescein 5(6)-isothiocyanate (FITC, 96%), 4′, 6′-diamidino-2-phenylindole dihydrochloride (DAPI), paraformaldehyde (PFA, 95%), Nile red (NR, 95%) were purchased from Aladdin Chemistry Co., Ltd. (Shanghai, China). Methyl thiazolyl tetrazolium (MTT), lipopolysaccharides (LPS), and 2, 7-dichlorfluorescein diacetate (DCFH-DA, 97%) were sourced from Sigma-Aldrich (Shanghai, China). Fetal bovine serum (FBS) and Dulbecco's modified Eagle's medium (DMEM) were obtained from Gibco (Grand Island, NY, USA). Hoechst 33342 staining solution and lysoGreen were ordered from Beyotime Biotechnology (Shanghai, China) and KeyGEN BioTECH (Jiangsu, China), respectively. Human Ox-LDL was purchased from Yiyuan Biotechnologies (Guangzhou, China), Oil Red O was obtained from Solarbio. All other chemicals were analytical grade (> 98.0 wt %) and used as received unless stated otherwise.

Synthesis of the -0.5G PAMAM

PAMAM was synthesized by the divergent method and involved a two-step iterative reaction sequence using Michael addition and amidation reactions to gradually diverge towards periphery that produced concentric shells of branch cells (generations) around a central initiator core [1]. Firstly, anhydrous methanol (200 mL) containing methyl acrylate (MA, 146 mL, 1.6 mol) was dropped into ethylenediamine (EDA, 13 mL, 0.2 mol) with an ice bath for 30 min, and the reaction was allowed to continue at 37 °C for 18 h under the protection of N_2. Finally, the methanol and excess MA were removed by rotary evaporator, and after dried under vacuum for 24 h, a pale yellow viscous liquid was obtained (-0.5G PAMAM, 79 g, 97%).

Synthesis of the 0G PAMAM

The anhydrous methanol containing EDA (140 mL, 2.1 mol) was slowly dropped into the methanol solution (150 mL) that containing -0.5G PAMAM (35 g, 0.087 mol) under ice bath conditions and stirred for 20 min. After the reaction was stirred at 35 °C for 24 h, removing the methanol and unreacted EDA by rotary evaporator, and further vacuum drying for 24 h to obtain a light yellow viscous liquid (0G PAMAM, 43 g, 96%).

Synthesis of the 0.5G PAMAM

Under ice-bath conditions, the methanol solution (150 mL) containing 0G PAMAM (36 g, 0.07

mol) was added dropwise to anhydrous methanol containing MA (223 mL, 2.4 mol) over a period of 20 min. After that, the reaction was carried out at 35 °C for 24 h, followed by removing the methanol and unreacted MA with rotary evaporator, and a light yellow viscous liquid (0.5G PAMAM, 81 g, 97%) was obtained after vacuum drying for 24 hours.

Synthesis of the 4.0G PAMAM

The preparation process of 1.5G, 2.5G and 3.5G PAMAM was the same as that of 0.5G PAMAM, while the preparation process of 1.0G, 2.0G, 3.0G and 4.0G PAMAM was the same as that of 0G PAMAM. The dosages of MA and EDA were increased proportionally, and the reaction time was correspondingly prolonged, as shown in Table 1.

Table 1. The ratio, reaction time and yield for each generation PAMAM

Generation	PAMAM/g	MA/mL	EDA/mL	T/h	$Mw_{dialysis}$/Da	yield/%
1.0G	0.5G/60	-	160	24	1000	95.0
1.5G	1.0G/30	138	-	36	1500	99.9
2.0G	1.5G/40	-	76	48	3000	98.3
2.5G	2.0G/40	108	-	48	5000	94.7
3.0G	2.5G/50	-	71	72	6000	97.5
3.5G	3.0G/40	68	-	72	10000	96.8
4.0G	3.5G/50	-	74	96	12000	91.2

$Mw_{dialysis}$: The Mw of dialysis bags.

Synthesis of the PAM-SH

The PAM-SH was prepared as previously described with modifications [2]. Specifically, 0.04 g 2-iminothiolane hydrochloride was added to 50 mL PBS (pH = 8, 0.001M EDTA) containing 0.5 g 4.0G PAMAM. The reaction was carried out under N_2 atmosphere and dark conditions for stirring at room temperature overnight. After dialysis against deionized water (9×3 L) with dialysis membranes (MWCO 1.0 kDa) for 48 h and further freeze-dried with a lyophilizer (Biocool Ltd., Lab-1A-50, China), the white flocculent solid (PAM-SH, 0.613 g) was obtained.

Synthesis of the SA PAM

The SA PAM were prepared by the DMSO-induced self-assembly of PAM-SH and SA. SA was synthesized by ring opening of simvastatin lactone according to a literature that previously reported [3]. Briefly, NaOH (17 mL, 0.1 M) was added to 11 mL ethanol containing 0.456 g simvastatin and reacted at 50 °C for 2 h, followed by adjusting the pH of the solvent to neutral with HCl. The solvent was removed by rotary evaporator and the residue was dissolved in deionized water. After added n-butanol to extract SA, the organic layer was collected and removed by rotary evaporator, and further vacuum drying to harvest 0.402 g SA. Subsequently, we prepared SA PAM with a 5:10 mass ratio of PAM-SH to SA. NaBH4 (0.5 mL, 0.1 M) was added to deionized water containing 5 mg PAM-SH and stirred at room temperature for 3 h under N2 atmosphere, the solution was adjusted to neutrality with 0.1 M HCl. After that, 2 mL DMSO solution containing 10 mg SA was slowly dropped into the solvent, and the reaction was allowed to continue at room temperature for 5 h. Finally, the -S-S- crosslinked SA PAM was obtained via dialyzed (MWCO 1.0 kDa) in deionized water for 2 days. We used the same method to prepare SA PAM with different mass ratios (PAM-SH : SA = 3:10, 10:10, 20:10, 30:10).

Synthesis of the SA PAM@RBCs

RBCs were extracted according to the previous literature with modifications [4]. 4 mL fresh whole blood from the corresponding animals was charged into a centrifuge tube containing 3.8% sodium citrate, which was centrifuged (2000 r/min, 10 min) at 4 °C to remove plasma, platelets and buffy coat for isolate erythrocytes. RBCs were washed with sterile isotonic phosphate-buffered saline (1×PBS) 4 times to discard the supernatant, followed by resuspending the RBCs in PBS for succeeding use. A dose of SA PAM was added to the diluted RBCs to incubate for 1 h at room temperature and centrifugated to obtain the SA PAM@RBCs [5].

Characterization of SA PAM and SA PAM@RBCs

The chemical structure of 4.0G PAMAM, PAM-SH and SA were analyzed using fourier transform infrared spectroscopy (FT-IR, Nicolet iS10, Thermo Scientific Co. Ltd., USA) and ^{1}H NMR spectrum (Bruker, Germany, 300 MHz) with $CDCl_3$ as the solvent. The molecular weight of the entire generation of PAMAM was characterized by MALDI-TOF MS (Bruker, Germany, Autoflex speed TOF/TOF). The grafting rate of sulfhydryl groups in 4.0G PAMAM was calculated using the L-cysteine standard curve as the previously reported. The morphology and size of 4.0G PAMAM, PAM-SH and SA PAM were investigated with high-resolution TEM (JEM-2100F, JEOL Ltd, Japan) and ZetaPlus (Brookhaven Co., Ltd., USA). The zeta potential and partical size of SA PAM were measured by the ZetaPlus. Scanning electron microscope (SEM, SU8100, HITACHI Ltd., Japan) and UV-visible spectrometer (UH4150, HITACHI Ltd., Japan) were used to record the morphology and safety of SA PAM@RBCs [6, 7].

Determination of the Thiol Group Content

To verify the introduction of sulfhydryl groups in 4.0G PAMAM, Ellman test was carried out according to the previous scheme [8, 9]. Ellman's test principle is using the color reagent 5, 5'-dithiobis-(2-nitrobenzoic acid) (DTNB, also known as Ellman's reagent) to react with thiol to generate a molecule 2-nitro-5- thiobenzoic acid (TNB) that has a strong absorption peak at 412 nm. Briefly, 0.01 g PAM-SH was dissolved into 5 mL sodium phosphate buffer (0.1 M, pH 7.2) that containing 1 mM EDTA, 1 mL above solution was mixed with 3 mL DTNB (0.1 mM) and reacted at room temperature for 15 min. The solution absorbance was measured at 412 nm using a Hitachi UH4150 spectrophotometer and calculated the amount of sulfhydryl groups based on the standard curve of L-cysteine.

Drug loading and release

The SA content in the SA PAM was detected in PBS (pH 7.4) containing H_2O_2 with a UV-visible spectrometer (UV-2450, SHIMADZU Ltd., Japan) at 243 nm. After lyophilizing the SA PAM solution, a realistic amount of SA PAM powder was weighed to dissolve in PBS that containing H_2O_2, and the supernatant was transferred to a quartz cuvette after centrifuged at high speed to observe the ultraviolet absorption peak at 25 °C. The drug loading content was obtained according to the established standard curve [10]. The in vitro drug release studies were conducted using dialysis bags. In brief, the equivalent amount of SA PAM solution which was packed into the dialysis bag (MWCO 3.5 kDa) was immersed in PBS containing different concentrations of H_2O_2 (0, 2.5, 5, 7.5 to 10 mM) and the whole volume was 68 mL in each sample. The experiments were placed on a gently strring platform in the dark at 37 °C. At predetermined time points, 3 mL dialysate

was withdrawn for UV determination to quantify SA, while adding an equal volume of fresh dialysate to keep the volume constant. DLS was used to monitor the change in particle size of SA PAM at 24 h, 48 h and 72 h. We changed the above-mentioned PBS that containing different concentrations of H2O2 to PBS at pH 5 and 7.4 without H2O2, and further tested the SA release of SA PAM due to pH-sensitive. All data were presented in average with the tests were repeated thrice. The drug loading (DL) and entrapment efficiency (EE) were calculated using the following formula [11, 12].

$$DL(\%) = \frac{mass\ of\ SA\ in\ SA\ PAM}{mass\ of\ SA\ PAM} \times 100\%$$

$$EE(\%) = \frac{mass\ of\ SA\ in\ SA\ PAM}{mass\ of\ drug\ added\ initially} \times 100\%$$

Cells and animals

The human umbilical vein endothelial cells (HUVEC) and RAW 264.7 were cultured with complete DMEM solution that containing 1% penicillin–streptomycin and 10% fetal bovine serum. These cells were incubated into the 37 °C incubator including 5% CO_2. Male New Zealand white rabbits (2000 ± 100 g, Liaoning, China), male ApoE$^{-/-}$ deficient mices (8-10 weeks old, 20 ± 5 g), male Sprague-Dawley rats (SD, 200 ± 20 g) and male Kunming mices (KM, 10 weeks old, 20 ± 5 g) were obtained from Beijing Weitong Lihua Experimental Animal Technology Co., Ltd. The animals were housed in the specific pathogen free (SPF) animal room at 20 °C for 3 days with ad libitum access to water and food before experiments.

Hemocompatibility evaluation

The hemolytic activity of SA PAM was performed as the previously reported procedure with some modifications [13]. Briefly, fresh blood obtained from rabbits was charged into centrifuge tube containing anticoagulant sodium citrate and then centrifuged immediately at 2000 rpm for 10 min to discard the supernatant containing the plasma and leukocytes to obtain the RBCs. The obtained RBCs were washed three times with PBS (pH 7.4) until the supernatant was clear and then resuspended in PBS. The RBCs suspension (100 μL) was co-incubated with SA PAM in different concentrations for 1 h at 37 °C. In this study, we tested the PAM-SH hemolysis at seven concentrations (0, 2, 4, 6, 8, 16, 24, 32, 38 μg/mL) and the drug hemolysis of SA PAM at another seven concentrations (0, 2, 4, 6, 8, 10, 16, 24 μg/mL). After incubation, the mixture was centrifuged at 2000 rpm for 10 min. The resulting supernatant was analyzed at 540 nm using the UV–vis spectroscopy to measure the hemoglobin release. Untreated RBCs as negative control (0% hemolysis) while the RBCs treated with deionized water as positive control (100% hemolysis). The hemolytic response was evaluated using the following formula:

$$Hemolysis(\%) = \frac{A_{sample} - A_{negative}}{A_{positive} - A_{negative}}$$

Cytotoxicity studies

In vitro safety of PAM-SH and SA PAM was measured with RAW 264.7 and HUVECs via MTT assay, respectively. In brief, each cell line was placed in 96-well plates at a density of 5×10^3 cells/well and incubated at 37 °C overnight in humidified atmosphere with 5% CO_2. After that, the cells were treated with PAM-SH and SA PAM in various concentrations (0, 0.125, 0.25, 0.5, 1, 2,

4, 8, 16, 32, 64 μg/mL) for 24 h and 20 μL MTT was added to each well under dark conditions to continue incubating for another 4 h. Finally, the medium was discarded carefully and 150 μL DMSO was added to dissolve the formed formazan crystal. The absorbance of each well at 492 nm was obtained with a plate reader (SpectraMax 340PC, Molecular Devices, USA), and the effect of PAM-SH and SA PAM on cell viability was evaluated using the cell survival formula as follows [14, 15]:

$$Cell\ viability\ (\%) = \frac{OD_s - OD_b}{OD_C - OD_b} \times 100\%$$

where OD_s and OD_C denote the absorbance of the sample and the solvent control (DMEM medium), respectively. OD_b present the absorbance of DMEM medium without cells.

ROS levels of SA PAM in vitro

The intracellular ROS levels of RAW 264.7 were measured by using the DCFH-DA. After the acetate group is hydrolyzed by intracellular esterase and subsequently oxidized by ROS, DCFH-DA is converted to the 2′,7′-dichlorofluorescein (DCF) with green fluorescence, and the fluorescence intensity is directly proportional to the level of ROS [16]. Briefly, RAW 264.7 cells were seeded at a density of 1×10^5 cells per well in laser confocal petri dish and treated with LPS (4 μg/mL) at 37 °C for 36 h. The culture media was replaced with fresh media containing SA (4 μg/mL) or SA PAM (4 μg/mL) after the cells were washed with PBS buffer thrice. After exposed to SA or SA PAM for a period of time, the cells were washed three times and incubated with 10 μM DCFH-DA in the dark for another 30 min. The fluorogenic probe solution was then replaced with Hoechst 33342 (1 mM) to continue staining for 5 min. The fluorescence levels of RAW 264.7 were assessed with confocal laser scanning microscopy (CLSM, Zeiss LSM 780, Germany) [17, 18].

Flow cytometry analysis

According to the "Intracellular ROS detection" procedure, after incubating SA or SA PAM with RAW 264.7, cells were treated with 10 μM DCFH-DA for 30 min and washed three times by PBS buffer to adjust the cell concentration to 2×10^6 /mL, and the intensity of fluorescence were recorded by flow cytometry (BD FACSCelesta, USA).

In vitro cellular uptake Study

The cellular uptake of NR PAM@RBCs (NR was used instead of SA) was conducted as the previously reported procedure with some modifications [19, 20]. Specifically**,** the RAW 264.7 cells were seeded in 6-well plates (2.0×10^5 cells/well) containing DMEM and incubated at 37 °C until 80-90% confluence. The medium was aspirated and cells were washed three times with PBS buffer before cells were treated with NR PAM@RBCs (NR concentration 50 μg/mL) at 37 °C with the final concentration was 1 μg/mL. After the respective time points, the cells were gently washed twice with ice-cold PBS buffer to remove NR PAM@RBCs and stained lysosome with LysoGreen dye for 1 h at 37 °C. Before imaging, the cells were fixed with 4% PFA for 20 min and the nuclei were stained with DAPI at room temperature in dark environment for 5 min and washed with PBS buffer. The fluorescence distribution was observed using CLSM and the fluorescence intensity was quantified using ImageJ.

The foam cells formation and the intracellular lipid droplets measurement

To detect the lipid droplets formation in foam cells, as described by Wang et al.[21-24], the RAW

264.7 cells were cultured on cover slips in 6-well plates (1×10^6 cells/well) overnight and treated with Ox-LDL (50 μg/mL) in the presence or absence of SA (4 μg/mL), PAM-SH (5 μg/mL) or SA PAM (4, 10 μg/mL) for 48 h. The cells were fixed with 4% PFA for 30 min and stained with Oil Red O at room temperature for 1 h. After washing 3 times with PBS, the cells with red lipid droplets were observed and photographed using an inverted microscope (MoticAE2000, China).

In vitro shear model

In order to prove the nanoparticles at the thrombus site could fall off from the red blood cell surface under flow conditions, we used FITC, which was convenient for observation, instead of SA to form nanoparticles (FITC PAM). The FITC PAM was adsorbed to the red blood cells surface (FITC PAM@RBCs) whose membrane has been labeled with NR for observing the adsorption of nanoparticles on the erythrocyte membrane using CLSM after shearing. In this study, the radial peristaltic pump was used to simulate the heart providing pulsatile flow and generating shear forces during blood circulation. Another advantage of the radial peristaltic pump was that the drug solution was only in direct contact with the pipeline and not directly with the pump itself, which would minimize the interference of solution contamination and other influencing factors on the results obtained [25]. The medical silicone tube (1.6 mm in diameter and 1 m in length) was used to replace the blood vessel while the non-plug syringe was used as a solution reservoir. The above three parts were connected to form a cardiovascular circulatory system model, and the simulation of the thrombosis site was realized by a plexiglass box sleeved on the outside of the silicone tube. The nut on the plexiglass box was used to control the shear force by controlling the radius of the silicone tube to realize the in vitro simulation of the shear force at thrombus site [26].

Before conducting the experiment, sterilized the entire system with 75% ethanol and rinsed with PBS buffer for 2 min to remove the ethanol. In order to prevent the erythrocytes adhere to the inner wall of the silicone tube, the channel was incubated with 2% bovine serum albumin (BSA, Sigma) for 10 min. Subsequently, 5 mL FITC PAM@RBCs suspension was added to the syringe and incubated at 37 °C, the pump parameters were setted according to Poiseuille's law and the inner diameter of the silicone tube was adjusted using gaskets to achieve the shear stress (τ) to 2 Pa (20 dynes/cm^2) that represented the shear stress of healthy blood vessels or 10 Pa (100 dynes/cm^2) that represented the shear stress at the thrombus site. After circulating for a certain period of time, the suspension was collected and the adsorption of nanoparticles on erythrocyte were observed using CLSM. The red fluorescence of the cells and the green fluorescence of the nanoparticles were quantitatively determined by analyzing each cell in the acquired images using ImageJ. This experiment only study the desorption of FITC PAM@RBCs under the action of shear stress reported in the literature on healthy blood vessels and thrombus site. The purpose is to prove that FITC PAM@RBCs is responsive to shear stress, not to study the changes in the desorption amount of FITC PAM from RBCs as the shear stress increases, so no more shear stress is tested. The Poiseuille's law as follows [27]:

$$\tau = \frac{4\mu Q}{\pi R^3}$$

where μ is the viscosity coefficient of PBS solution containing 2% BSA (0.01 dynes/cm^2), Q stands for volume flow rate (from 0.027 to 27 mL/min), and R represents the radius of the silicone tube (0.8 mm).

Pharmacokinetics

A single dose of free SA and nanomedicines were injected through the tail vein at a dose of 20 mg/kg body weight. Blood was sampled from the retro orbital plexus of rats into a centrifuge tube containing anticoagulant at predetermined time points (0.083 h, 0.25 h, 0.5 h, 1 h, 3 h, 6 h, 12 h and 24 h) after injection, and centrifuged at 4000 r/min for 10 min to obtain the plasma. SA plasma concentrations were measured by UV.

A $FeCl_3$-induced carotid thrombosis rabbit model

The carotid thrombosis was induced by $FeCl_3$ as previously described with some modifications [28]. After the rabbits were anesthetized with pentobarbital sodium (3%, 40 mg/kg), the left common carotid arteries were exposed for recording the blood flow using an ultrasonic Doppler flow probe (EPIQ7C, Royal Philips Inc., Netherlands). Warpping around the carotid arteries with a filter paper saturated containing 30% $FeCl_3$ to induced thrombosis and the SA, SA PAM, or SA PAM@RBCs was injected simultaneously. After the carotid arteries injuried, the filter paper was removed and the state of blood flow was recorded using the ultrasonic Doppler flow probe for 30 min. Thereafter, the rabbits were sacrificed to harvest the carotid arteries, which were stained with H&E for observing the thrombus formation, and the thrombosis area was analyzed using imageJ software. We also gathered the thrombosis-induced carotid arteries for comparing the weight and length after the thrombosis was dried. Finally, we used DCFH-DA to detect the ROS levels in the plaque.

ApoE$^{-/-}$ mices model

After three days of acclimatization with an ordinary chow diet, the ApoE$^{-/-}$ mices were randomly divided into 4 groups (control, SA, SA PAM and SA PAM@RBCs groups). The mices were fed with high-fat diet for 24 weeks and received therapy every three days during the last 8 weeks in a dose of 80 mg/kg. All mices were sacrificed after the last treatment for 24 h, and the aortic arches were harvested for examining the lipid deposition via Oil red O staining to evaluate the effect of SA PAM@RBCs on thrombosis. We also quantitatively analyzed the area of lipid deposition using imageJ software [29].

In vivo fluorescence imaging

Cy7 instead of SA to obtain Cy7 PAM@RBCs for fluorescence imaging in the same way as that of preparing SA PAM@RBCs. After 24 weeks high-fat feeding, ApoE$^{-/-}$ mice were injected with Cy7 PAM@RBCs via the tail vein at a dose of 1 mg/kg body weight. The mice were sacrificed at a predetermined time point to obtain the heart, liver, spleen, lung, kidney, and aorta. Fluorescence images of the main organs and separated aortas were taken on a small animal in vivo fluorescence imaging system (IVIS lumina Xr, USA). The same experiments were performed with free Cy7 and Cy7 PAM as controls.

Safety evaluation

Healthy KM mices were intravenously injected with saline, SA, SA PAM or SA PAM@RBCs (80 mg/kg) every three days. The blood samples were harvested from the ocular vein to assess the coagulation indicators, liver and kidney function after half a month administration. The major tissues (heart, spleen, kidney, liver and lung) were obtained for H&E staining after the mice were sacrificed.

Statistical analysis

Statistical analysis are conducted with GraphPad Prism software and all results are presented as mean ± standard deviation. The statistical differences between groups are analyzed by student's t-test and $P<0.05$ was considered statistically significant.

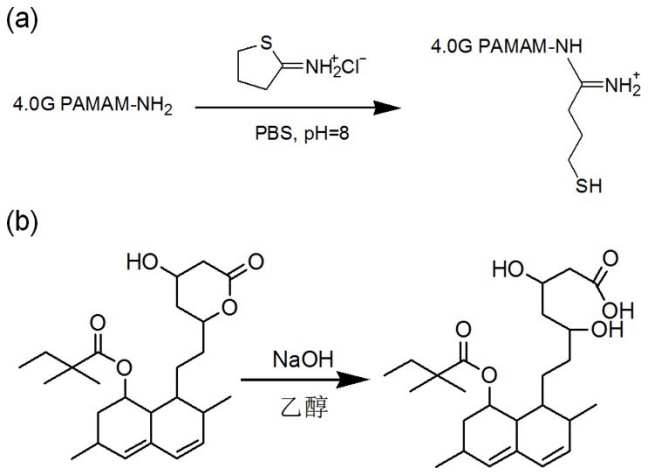

Figure S1. The synthesis of PAM-SH (a) and simvastatin acid (b).

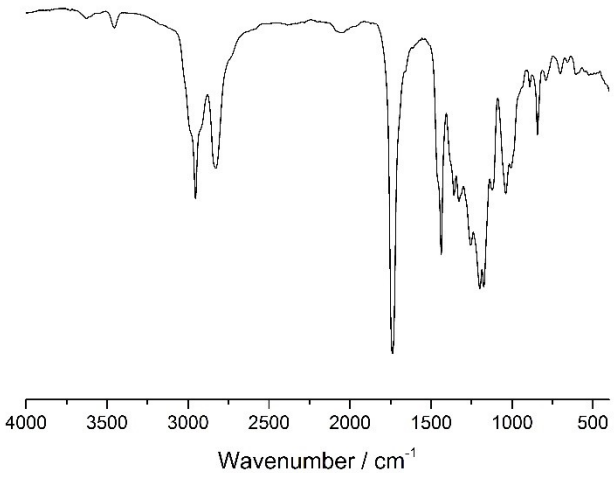

Figure S2. The FTIR spectra of -0.5G PAMAM.

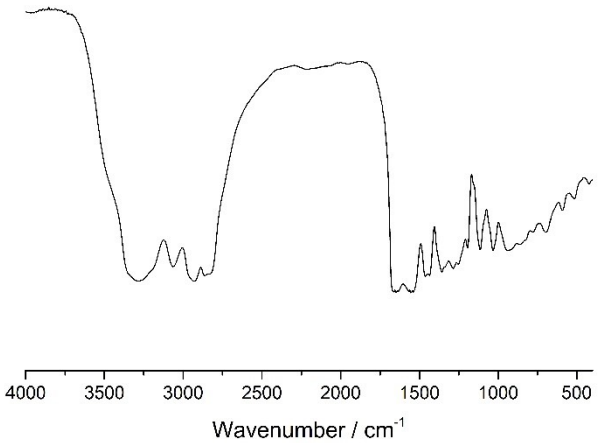

Figure S3. The FTIR spectra of 0G PAMAM.

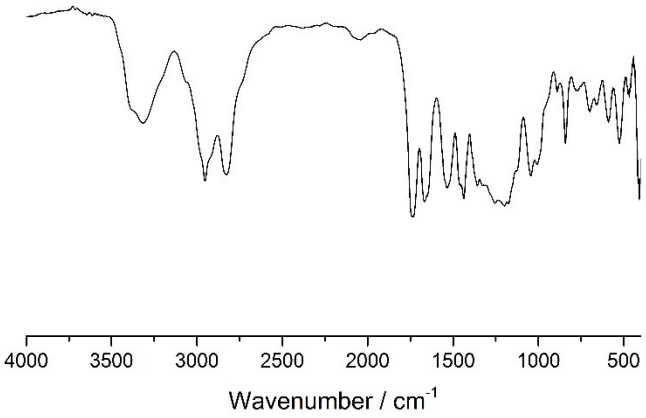

Figure S4. The FTIR spectra of 0.5G PAMAM.

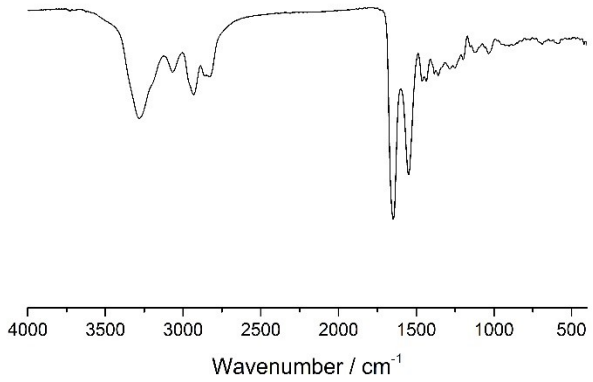

Figure S5. The FTIR spectra of 1.0G PAMAM.

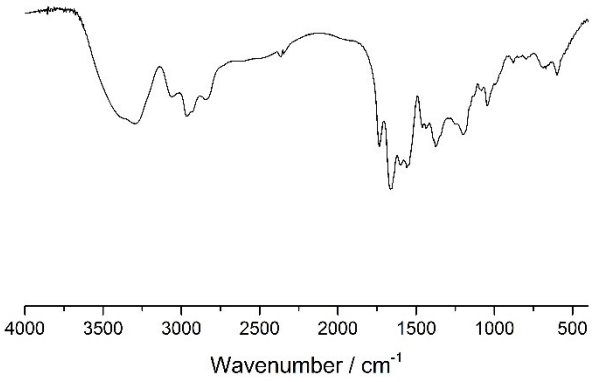

Figure S6. The FTIR spectra of 1.5G PAMAM.

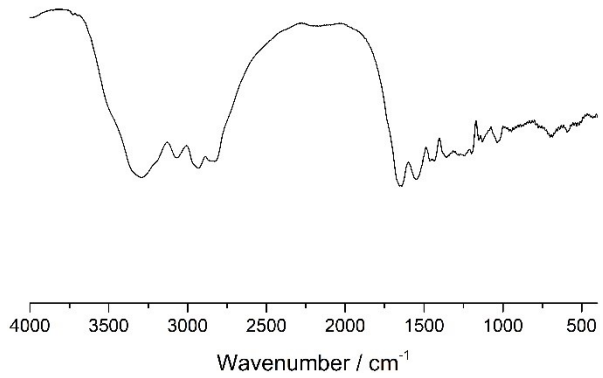

Figure S7. The FTIR spectra of 2.0G PAMAM.

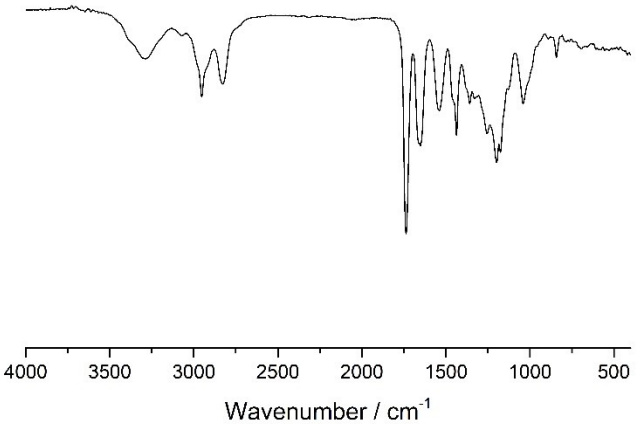

Figure S8. The FTIR spectra of 2.5G PAMAM.

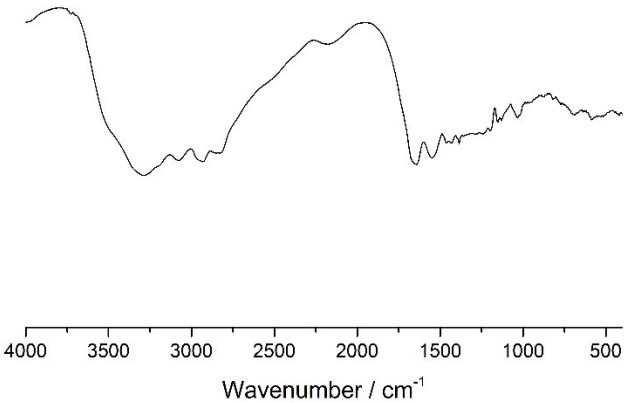

Figure S9. The FTIR spectra of 3.0G PAMAM.

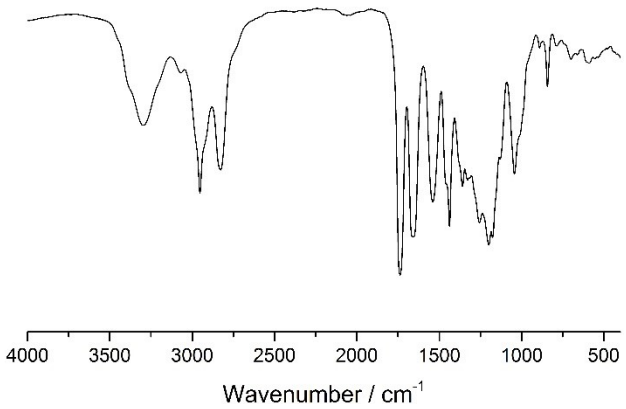

Figure S10. The FTIR spectra of 3.5G PAMAM.

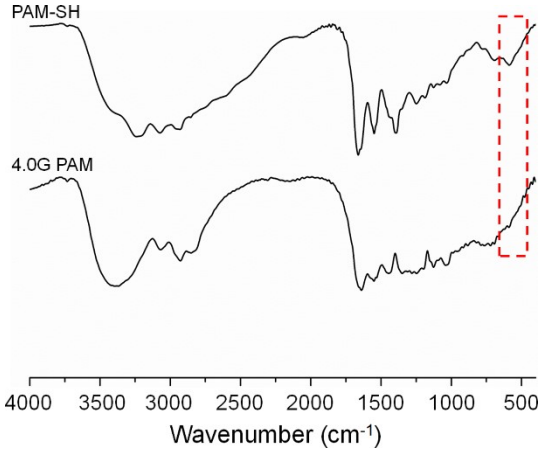

Figure S11. The FTIR spectra of 4.0G PAMAM and PAM-SH.

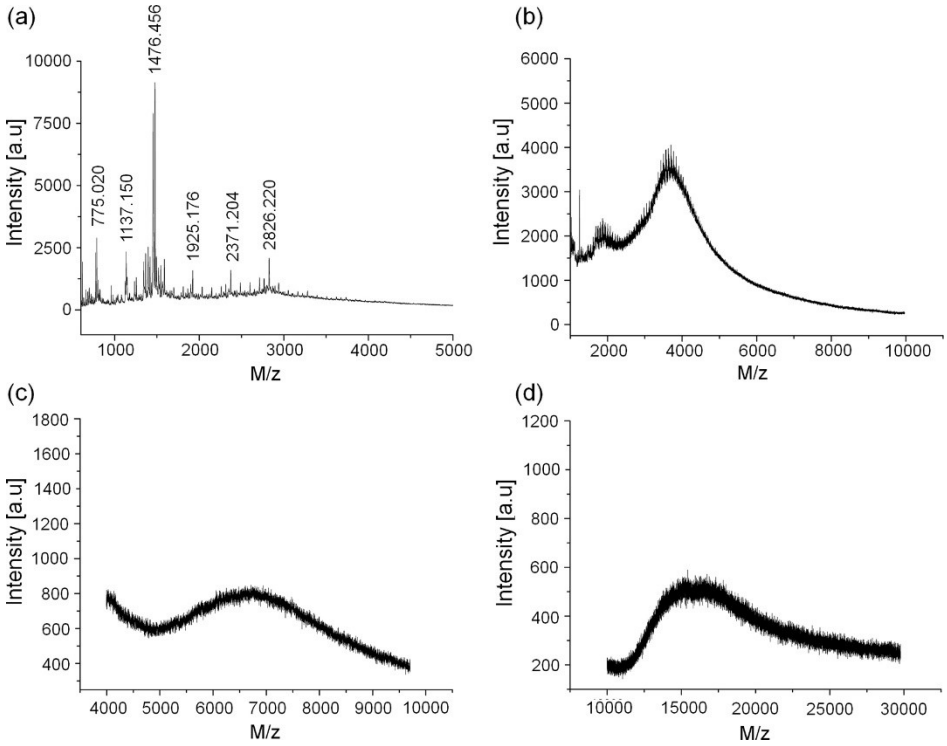

Figure S12. The MALDI-TOF MS of 1.0G PAMAM (a), 2.0G PAMAM (b), 3.0G PAMAM (c) and 4.0G PAMAM (d).

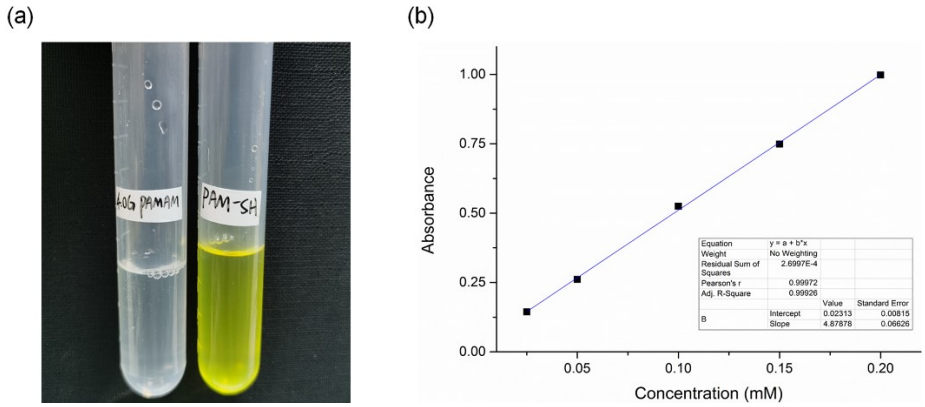

Figure S13. (a) The color comparison diagram of PAM-SH and 4.0G PAMAM solutions after adding Ellman's reagent; (b) The standard curve of L-cysteine.

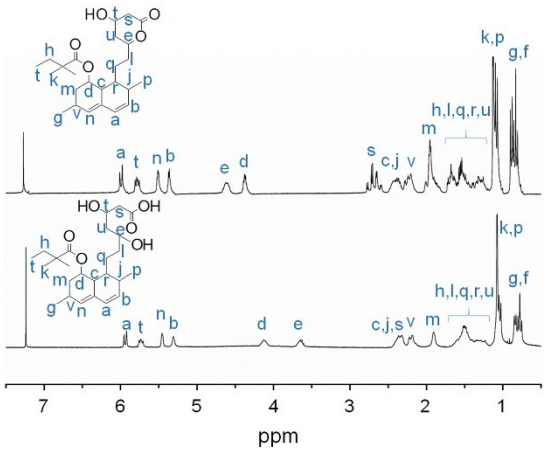

Figure S14. The ^{1}H NMR spectra of SA and simvastatin.

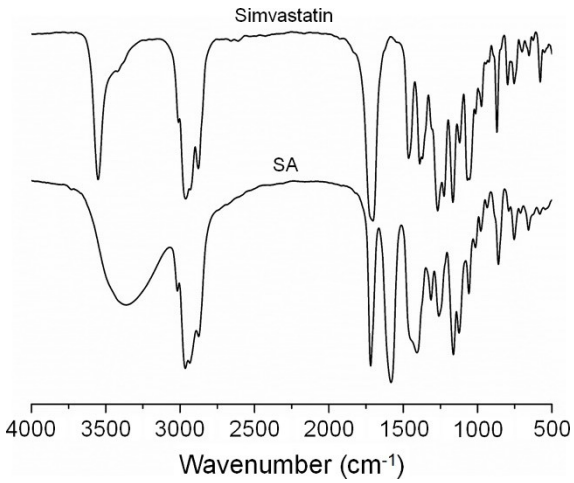

Figure S15. The FTIR spectra of SA and simvastatin.

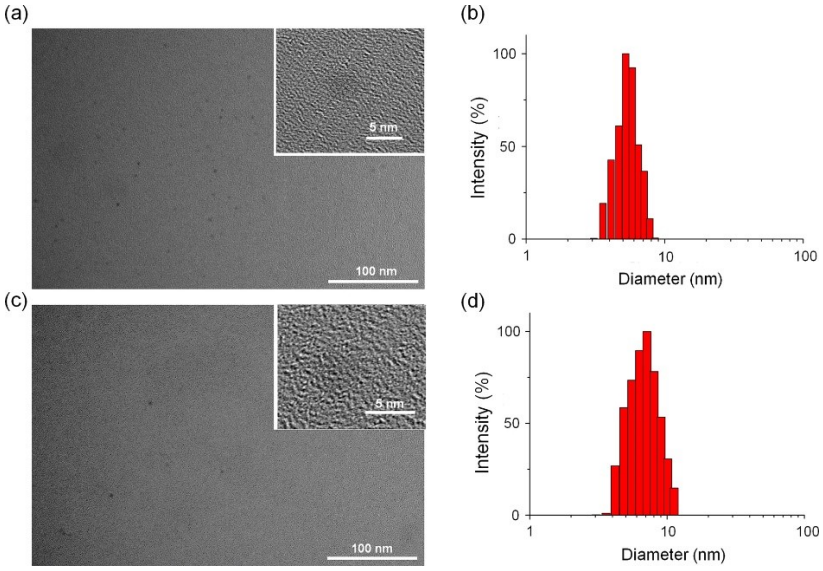

Figure S16. The morphology and size of 4.0G PAMAM and PAM-SH. (a) The TEM of 4.0G PAMAM; (b) The DLS of 4.0G PAMAM; (c) The TEM of PAM-SH; (d) The

DLS of PAM-SH.

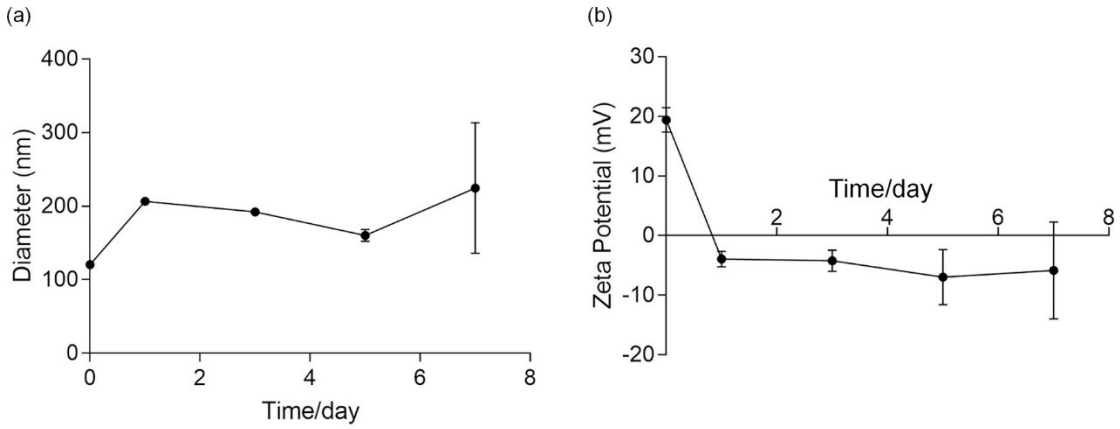

Figure S17. The size (a) and zeta potential (b) stability of SA PAM in serum within 7 days.

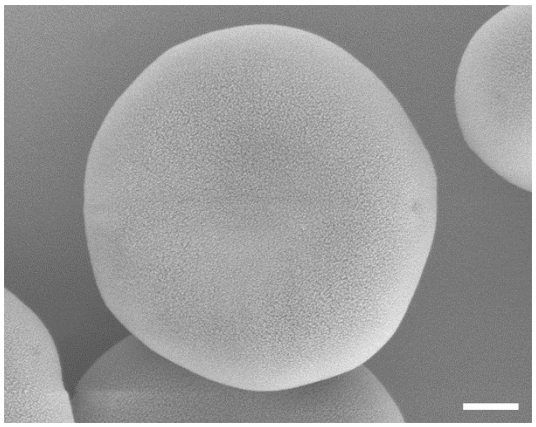

Figure S18. The SEM of individual RBCs.

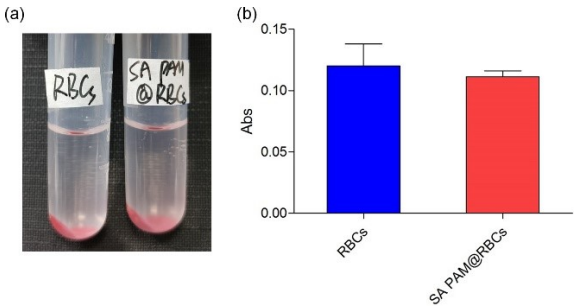

Figure S19. The safety of SA PAM (8 μg/mL) on RBCs. (a) The image of RBCs and SA PAM@RBCs after centrifugation. (b) The UV absorption intensity of RBCs and SA PAM@RBCs (n=3).

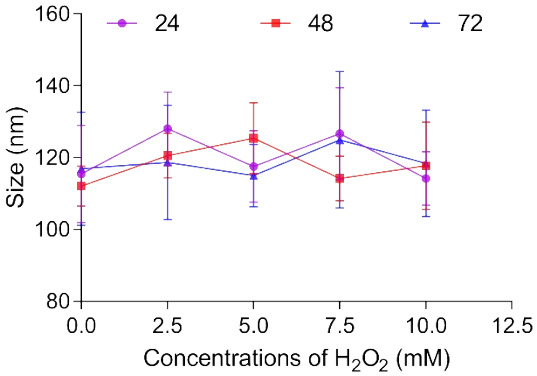

Figure S20. The change of SA PAM in term of size in different H_2O_2 concentrations at 24 h, 48 h and 72 h.

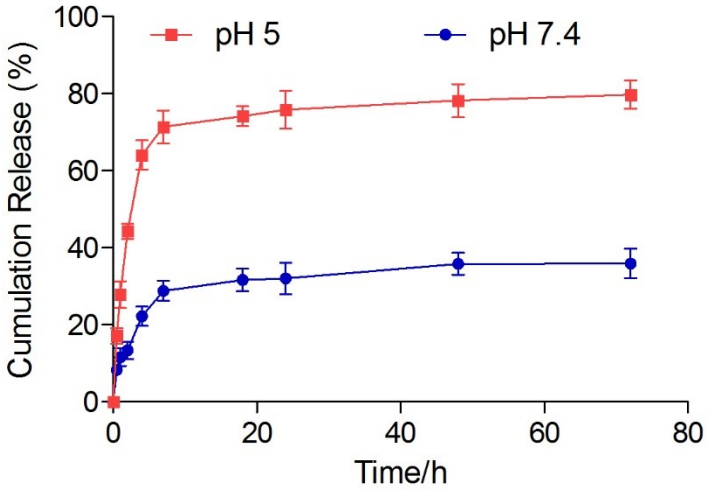

Figure S21. In vitro cumulative release profiles of SA from SA PAM in PBS at pH 5 and pH 7.4 (n = 3).

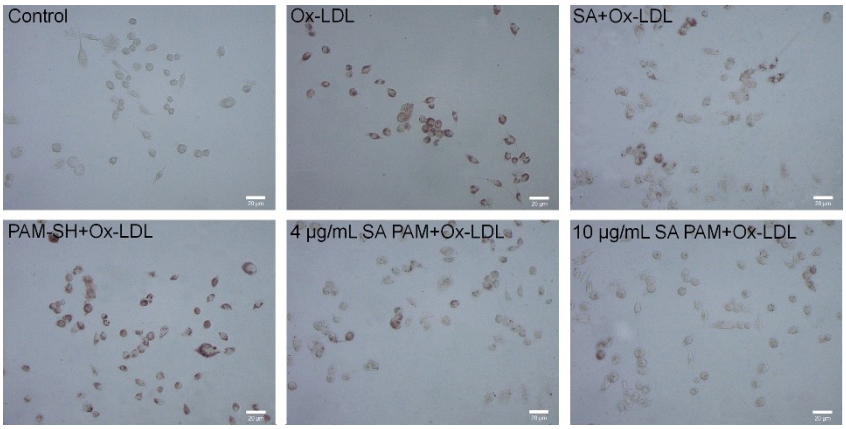

Figure S22. The effect of SA (4 μg/mL), PAM-SH (5 μg/mL) and SA PAM (4, 10 μg/mL) on foam cell formation induced by Ox-LDL (50 μg/mL) in RAW 264.7 cells. Representative images showing RAW 264.7 cells srained with Oil red O were harvested by inverse microscopy (Bar = 20 μm).

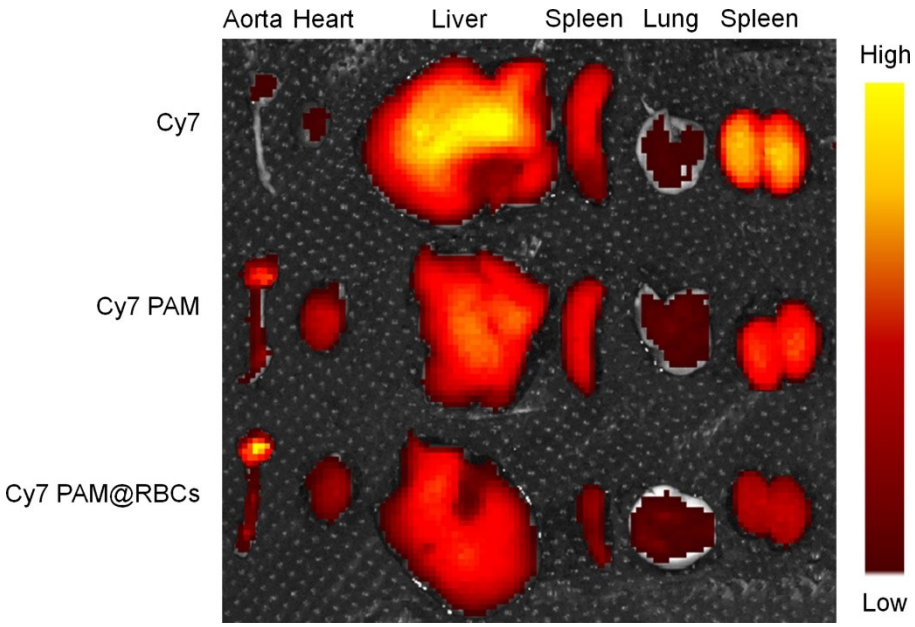

Figure S23. Ex vivo fluorescence imaging of the separated aortas and organs after ApoE-/- mices received tail vein injection of Cy7, Cy7 PAM and Cy7 PAM@RBCs.

Reference:

1. R. Kharwade, S. More, A. Warokar, P. Agrawal and N. Mahajan, *Arabian Journal of Chemistry*, 2020.
2. A. Braden, M. Roner, J. Ganter and K. Nelson, *J Nanosci Nanotechnol*, 2007, **7**, 925-936.
3. J. H. Jeon, M. V. Thomas and D. A. Puleo, *Int J Pharm*, 2007, **340**, 6-12.
4. Ú. Catalán, M.-Á. Rodríguez, M.-R. Ras, A. Maciá, R. Mallol, M. Vinaixa, S. Fernández-Castillejo, R.-M. Valls, A. Pedret and J. L. Griffin, *Mol Biosyst*, 2013, **9**, 1411-1422.
5. D. C. Pan, J. W. Myerson, J. S. Brenner, P. N. Patel, A. C. Anselmo, S. Mitragotri and V. Muzykantov, *Sci Rep*, 2018, **8**, 1-12.
6. S.-H. Park, J.-Y. Lee, H.-N. Cho, K.-R. Kim, S.-A. Yang, H.-J. Kim and K.-H. Jhee, *Journal of microbiology and biotechnology*, 2019, **29**, 114-126.
7. M. L. Sullivan and N. D. Bonawitz, *Plant Sci*, 2018, **269**, 148-152.
8. S. Zhang, S. Asghar, F. Yu, Z. Chen, Z. Hu, Q. Ping, F. Shao and Y. Xiao, *Journal of agricultural and food chemistry*, 2019, **67**, 9371-9381.
9. N. S. Gandhi, S. Godeshala, D.-L. T. Koomoa-Lange, B. Miryala, K. Rege and M. B. Chougule, *Pharm Res*, 2018, **35**, 1-20.
10. R. Ridolfo, J. J. Arends, J. C. van Hest and D. S. Williams, *Biomacromolecules*, 2020.
11. N. Selvasudha and K. Koumaravelou, *Carbohydr Polym*, **163**, 70-80.
12. X. Hou, H. Lin, X. Zhou, Z. Cheng, Y. Li, X. Liu, F. Zhao, Y. Zhu, P. Zhang and D. Chen, *Carbohydr Polym*, 2020, **232**.
13. Barbara, Crivelli, Elia, Bari, Sara, Perteghella, Laura, Catenacci, Milena and Sorrenti.
14. R. Wang, R. Wang, D. Chen, G. Qin and E. Zhang, *Journal of Alloys and Compounds*, 2020, **824**.
15. X. Hou, H. Lin, X. Zhou, Z. Cheng, Y. Li, X. Liu, F. Zhao, Y. Zhu, P. Zhang and D. Chen, *Carbohydr Polym*, 2020, **232**, 115787.
16. G. Agonigi, L. Biancalana, M. G. Lupo, M. Montopoli, N. Ferri, S. Zacchini, F. Binacchi, T.

Biver, B. Campanella, G. Pampaloni, V. Zanotti and F. Marchetti, *Organometallics*, 2020, **39**, 645-657.
17. H. Wu, F. Li and S. Wang, 2018, **151**, 66-77.
18. X. Chen, T. Wang, W. Le, X. Huang, M. Gao, Q. Chen, S. Xu, D. Yin, Q. Fu, C. Shao, B. Chen and D. Shi, *Theranostics*, 2020, **10**, 3430-3450.
19. J. Gao, P. Wu, A. Fernandez, J. Zhuang and S. Thayumanavan, *Angewandte Chemie-International Edition*, 2020, DOI: 10.1002/anie.202002748.
20. S. Maghrebi, P. Joyce, M. Jambhrunkar, N. Thomas and C. A. Prestidge, *ACS Appl Mater Interfaces*, 2020, **12**, 8030-8039.
21. Y. Wang, L. Li, W. Zhao, Y. Dou, H. An, H. Tao, X. Xu, Y. Jia, S. Lu and J. Zhang, *ACS Nano*, 2018, **12**, 8943-8960.
22. W. Gao, Y. Sun, M. Cai, Y. Zhao, W. Cao, Z. Liu, G. Cui and B. Tang, *Nat Commun*, 2018, **9**, 1-10.
23. V. Di Francesco, D. Gurgone, R. Palomba, M. F. M. M. Ferreira, T. Catelani, A. Cervadoro, P. Maffia and P. Decuzzi, *ACS Appl Mater Interfaces*, 2020, **12**, 37943-37956.
24. S. Hao, J. Ji, H. Zhao, L. Shang, J. Wu, H. Li, T. Qiao and K. Li, *Molecules*, 2015, **20**, 21287-21297.
25. T. Dreckmann, J. Boeuf, I.-S. Ludwig, J. Luemkemann and J. Huwyler, *Eur J Pharm Biopharm*, 2020, **147**, 10-18.
26. Y. Xin, X. Chen, X. Tang, K. Li, M. Yang, W. C.-S. Tai, Y. Liu and Y. Tan, *Biophys J*, 2019, **116**, 1803-1814.
27. E. Yeom, J. H. Park, Y. J. Kang and S. J. Lee, *Sci Rep*, 2016, **6**.
28. S. Subramaniam, S. Boukhlouf and C. Fletcher, *Blood Coagul Fibrinolysis*, 2019, **30**, 324-330.
29. F. Liu, S. Shan, H. Li and Z. Li, *Journal of Agricultural and Food Chemistry*, 2020.